European Journal of Neuroscience, Vol. 12, pp. 2367–2375, 2000

Retinal ganglion cells projecting to the nucleus of the optic tract and the dorsal terminal nucleus of the accessory optic system in macaque monkeys

I. Telkes, C. Distler and K.-P. Hoffmann
Allgemeine Zoologie & Neurobiologie, Ruhr-Universität Bochum, D44780 Bochum, Germany

Keywords: neuronal tract tracing, NOT-DTN, optokinetic system, retrograde transport

Abstract

Using classical neuroanatomical retrograde tracing methods we investigated the retinal ganglion cells projecting to the nucleus of the optic tract and dorsal terminal nucleus of the accessory optic system (NOT-DTN) in macaque monkeys. Our main aim was to quantify the strength of the projection from the ipsilateral retina to the NOT-DTN. We therefore examined the number, distribution, and soma size of retinal ganglion cells involved in this projection. Electrophysiologically controlled small injections into the NOT-DTN revealed a clearly bilateral retinal projection originating mainly from the central retina but also involving peripheral retinal regions. Labelled cells were found nasally in the contralateral retina and temporally in the ipsilateral retina with some overlap in the fovea. The projection from the ipsilateral retina was 36–43% of that from the contralateral retina. On average, only 1–6% of the local population of ganglion cells projected to the NOT-DTN. Small soma size and large dendritic fields imply that in monkey rarely encountered, 'specialized' ganglion cells provide the direct retinal input to the accessory optic system (AOS). These results are discussed with respect to the symmetry of monocular horizontal optokinetic nystagmus (OKN) in primates.

Introduction

The accessory optic system (AOS) of vertebrates is a functionally and morphologically well defined subsystem of the subcortical visual pathway. It consists of three terminal nuclei and interspersed cells receiving a highly specific retinal input (Simpson *et al*., 1988). In all the species investigated so far the retinal ganglion cells projecting to the AOS are direction selective (turtle, Rosenberg & Ariel, 1991; rabbit, Oyster *et al*., 1972; cat, Hoffmann & Stone, 1985). In monkey, this type of retinal ganglion cell has evaded discovery so far. However, monkeys (as all other mammals) have an AOS with three terminal nuclei (Cooper *et al*., 1990). It has been previously demonstrated that ganglion cells projecting to the direction selective cells in the pretectal nucleus of the optic tract and dorsal terminal nucleus of the accessory optic tract (NOT-DTN) have slowly conducting axons (Hoffmann *et al*., 1988), a property which would place them in the group of 'rarely encountered' or 'specialized' ganglion cells in this species.

A speciality of the monkey subcortical visual system is the strong ipsilateral retinal projection to the superior colliculus (SC), the pretectum and the AOS (Cooper *et al*., 1990; Kourouyan & Horton, 1997) which is much more prominent than in other mammals with frontal eyes, such as, e.g. cat (Berman, 1977; Hoffmann *et al*., 1984) or ferret (Zhang & Hoffmann, 1993). If a functionally strong ipsilateral visual input also exists to the NOT-DTN it could play an integral role in setting up and maintaining a symmetrical optokinetic reflex without the visual cortex (Hoffmann, 1983; Distler *et al*., 1999). By such a direct subcortical route each retina would be connected to retinal slip coding neurons necessary for leftward optokinetic nystagmus (OKN) on the left side and those necessary for rightward OKN on the right side of the midbrain. The data available so far come from anterograde tracing experiments in newborn and adult monkeys (Cooper *et al*., 1990; Kourouyan & Horton, 1997) and from retrograde labelling from the pretectum with subsequent intracellular fills of retinal ganglion cells in the primate retina (Rodieck & Watanabe, 1993). These studies demonstrate a strong ipsilateral retinal projection to the pretectum, or clearly describe the various morphological types of ganglion cells projecting to the pretectum but do not specify, how many and which type of ganglion cells terminate specifically in the contralateral and in the ipsilateral NOT-DTN. To answer the first question we made small injections of various retrograde tracers at physiologically identified recording sites of retinal slip cells in the NOT-DTN and analysed the number and distribution of ganglion cells labelled in the two retinae. The morphological type and whether the cells projecting to the NOT-DTN in the monkey retina are direction selective as in the turtle (Rosenberg & Ariel, 1991), the rabbit (Oyster *et al*., 1972; Pu & Amthor, 1990) or the cat (Hoffmann & Stone, 1985) remains to be elucidated.

Correspondence: Professor K.-P. Hoffmann, as above.
E-mail: kph@neurobiologie.ruhr-uni-bochum.de

Received 20 January 2000, revised 31 March 2000, accepted 3 April 2000

Materials and methods

Animals

Three normal adult monkeys, one female *Macaca fascicularis* (4–5 kg) and two male *Macaca mulatta* (6–7 kg), were used in the experiments. Monkeys received unilateral fluorescent tracer injections [Granular Blue, rhodamine–dextrane (MW3000) or horseradish peroxidase (HRP)/HRP conjugated to wheat germ agglutinin (WGA-HRP)] into the NOT-DTN at the termination of behavioural and electrophysiological investigations unrelated to the present study. All experiments were approved by the local ethics committee and were

carried out in accordance with the European Communities Council Directive of 24 November 1986 (S6609 EEC) and NIH guidelines for care and use of animals for experimental procedures.

Surgery and injections

The surgical methods have previously been described in detail (Hoffmann *et al*., 1988; Hoffmann & Distler, 1989). The animals were deeply anaesthetized with an initial intramuscular injection of ketamine hydrochloride (10 mg/kg). An intravenous catheter was inserted, and the monkeys were intubated through the mouth and placed into a stereotactic instrument. Throughout the experiment the animals were artificially ventilated with a mixture of nitrous oxide and oxygen as 3 : 1 and 0.3% halothane to maintain adequate anaesthesia. During surgery, animals received supplementary doses of pentobarbital as required. Heart rate, SPO_2, and blood pressure were recorded continuously, body temperature and end-tidal CO_2 were monitored and maintained at physiological levels.

To approach the NOT-DTN, the skin was cut, the skull exposed, and trephined at stereotactic coordinates (Snider & Lee, 1961; Szabo & Cowan, 1984) to allow access to the midbrain and pretectum. After electrophysiologically locating the NOT-DTN based on its location just lateral and anterior to the foveal representation in the superior colliculus (SC) and on its characteristic response properties (Hoffmann *et al*., 1988), a glass micropipette containing a recording wire and connected to a Hamilton microliter syringe via a short tube was advanced towards the NOT-DTN to verify the prospective injection site. Then, either 0.15 µL 2% Granular Blue (EMS-POLYLOY, Groβ-Umstadt) in distilled water, or 1 µL 15% rhodamine–dextrane (MW 3000; Molecular Probes, Leiden) in 0.1 M citrate NaOH (pH 3.0), or 0.5 µL 2% WGA-HRP (Sigma, Deisenhofen) with 10% HRP (Boehringer, Mannheim) in 0.1 M phosphate buffer pH 7.4 were slowly injected into one NOT-DTN of each of the three monkeys over a period of 20 min. After 20–30 min the pipette was withdrawn following aspiration. The wound was carefully closed in appropriate layers and the animals were allowed to recover. During the survival time, the animals received antibiotics and analgetics. In one case (WGA-HRP), the injection was performed at the beginning of an acute terminal experiment, and the animal remained anaesthetized over the whole survival period.

Histology

After an appropriate survival time (8 days after Granular Blue injection, 9 days after rhodamine–dextrane injection, and 58 h after WGA-HRP injection) the animals were deeply anaesthetized with an overdose of pentobarbital and perfused transcardially with 0.9% saline containing 0.1% procain hydrochloride followed by paraform-aldehyde–lysine–periodate (PLP) containing 4% paraformaldehyde (PFA). The eyes were removed from the skull, and small incisions were made in the sclera close to the ora serrata to facilitate diffusion. The eyes were then postfixed in PLP overnight. On the next day the retinae were removed from the eyeballs, and carefully dissected free of sclera, pigment epithelium, and vitreous body. The retinae labelled with Granular Blue or rhodamine–dextrane were mounted on slides, and covered in glycerol : PBS as 9 : 1. HRP was visualized using 3,3′,5,5′-tetramethylbenzidine (TMB; Sigma-Aldrich, Deisenhofen) as a chromogen (Mesulam, 1978; as modified from Van der Want *et al*., 1997).

For visualization of the injection sites, the midbrains were postfixed in PLP overnight, and, after cryoprotection in 10% and 20% glycerol, shock-frozen in isopenthane at –70 °C. Two alternate series of frontal, 40–50 µm thick frozen sections were cut on a microtome (Microm HM 500 OM), one for visualizing the neuronal tracers, the other for identifying subcortical nuclei in Nissl-stained material. The sections for analysing the location and spread of fluorescent tracers were mounted from 0.45% saline, dried on a hot-plate, defatted in xylene (2 × 1 min), and covered in DePex (Serva, Heidelberg). The WGA-HRP injection site was visualized using TMB histochemistry as described above.

Reconstruction of the injection sites

Camera-lucida drawings were made from Nissl-stained midbrain sections at a fluorescence microscope (ZEISS Axioskop). The location and the extent of the tracer injections were charted on these drawings of neighbouring sections.

Data analysis

To quantify the number and the size of the NOT-DTN projecting ganglion cells in the three animals we used a fluorescence microscope (ZEISS Axioskop) coupled to a computer-based reconstruction system (Neuron Tracing System, Eutectic Electronics, Inc., Raleigh, NC; 1995 version 5.1). The labelled ganglion cells were counted with a 40 × Neofluar objective, and the soma sizes were measured with a 100 × oil immersion objective. First, the outlines of the retinal whole-mounts were mapped and the locations of the fovea, optic disc, and individual labelled cells were marked. Then, the NOT-DTN projecting ganglion cells were counted and the ratio of projecting cells to the total cell number as given in the literature was calculated. The soma size of the NOT-DTN projecting ganglion cells was measured in different retinae at several retinal eccentricities and given in μm^2. No corrections were applied for shrinkage of the retinae because it was small.

Results

Injection sites

The location of the injection site, the tracer used, the survival time and the number of labelled ganglion cells for each animal is given in Table 1. We examined the area of spread of the tracer around the injection sites in Nissl-stained sections for indications of tissue damage due to the tracer, as well as in unstained (fluorescence tracer)

TABLE 1. Summary of NOT-DTN injection sites, tracers and resulting labelled ganglion cells

Animal	Species	NOT-DTN injection	Tracer	Labelled Pγ + Pε cells (Contralateral retina)	Labelled Pγ + Pε cells (Ipsilateral retina)	Ipsilateral to contralateral ratio
Case 1	*M. mulatta*	Right	WGA-HRP/10% HRP (0.5 µL 2%)	1077 (942) (1.2%)	1524 (396) (2.8%)	0.42
Case 2	*M. mulatta*	Left	Rhodamine–dextrane (1 µL 15%)	3378 (1.2%)	1227 (0.7%)	0.36
Case 3	*M. fascicularis*	Right	Granular Blue (0.15 µL 2%)	7496 (2.4%)	3220 (1.8%)	0.43

The table summarizes the cases, volume and concentration of the tracers used, the injection sites, the resulting number of labelled Pγ and Pε cells in the contralateral and the ipsilateral retina, and the mean percentage of labelled cells in relation to the local cell density (%), as well as the ratio of labelled ganglion cells in the ipsi- and contralateral retina. The numbers in parentheses (942, 396), in case 1, give the number of labelled cells outside the area indicated by a circle in Fig. 2, where the labelling in the contralateral retina was unsatisfactory.

and histochemically developed (WGA-HRP) sections. The reconstructions of the injection sites for each animal are shown in Fig. 1. The WGA-HRP/HRP injection into the right NOT-DTN of case 1 (Fig. 1A) was centred below the lateral edge of the brachium of the superior colliculus (BSC). The tracer spread to a small extent to the pulvinar (Pul); an obvious involvement of the superior colliculus was not evident from the inspection of the sections near the injection site. The rhodamine–dextrane injection into the left NOT-DTN in case 2 (Fig. 1B) was placed below the medio-lateral centre of the BSC. The injection was rather small, with little or no involvement of the pulvinar. However, involvement of the superior colliculus can not be wholly excluded. The Granular Blue injection into the right NOT-DTN in case 3 (Fig. 1C) was centred below the latero-posterior part of the BSC with some possible spread to the superior colliculus. With all injections we judged the involvement of the SC as negligible because there was no significant labelling of the dorsal retinae that could have been attributed to an involvement of the lateral SC representing the lower visual field. In all cases, injections were centred in the NOT-DTN and retrogradely labelled cells were found in the NOT-DTN contralateral to the injection site. Because it has been shown in other systems that different tracers may not be equally efficient in labelling neuronal connections especially when few terminals are involved (Güntürkün *et al*., 1993), we used three different tracers. Although the absolute number of labelled ganglion cells differed between cases, the distribution and ipsi- : contralateral ratio was similar; thus, it is unlikely that the choice of tracers had an aversive effect.

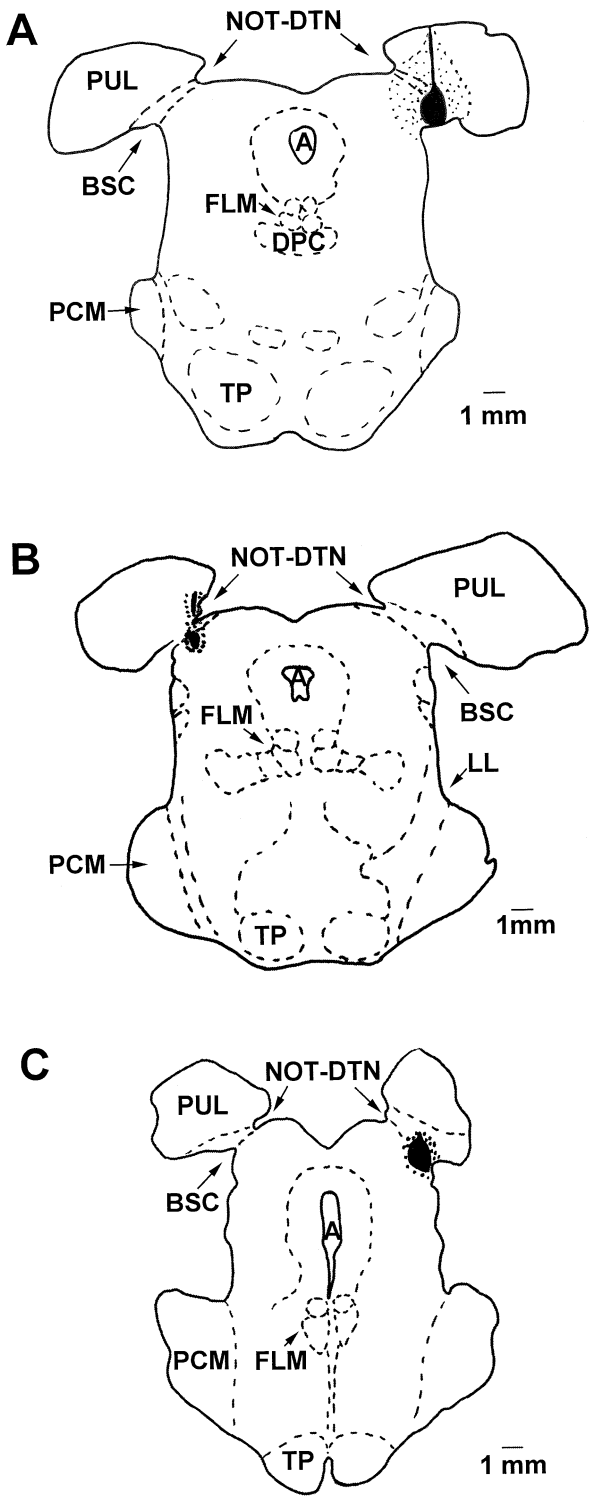

FIG. 1. Reconstruction of the injection sites in case 1 (A, WGA-HRP/HRP), case 2 (B, rhodamine–dextrane), and case 3 (C, Granular Blue) in frontal sections through the midbrain. The centre of the injections is given in black, dotted areas around the centre indicate the spread of the tracer. For abbreviations see list. Scale bars, 1 mm.

Distribution and number of retrogradely labelled ganglion cells

In all retinae it was obvious that only a small portion of the total number of retinal ganglion cells was labelled, as has been been described previously for the retinal projection to the pretectum and superior colliculus (Bunt *et al*., 1975; Perry & Cowey, 1984). The typical distribution of NOT-DTN projecting ganglion cells is shown for case 1 in Fig. 2. The labelled cells lie in the nasal portion of the contralateral retina and in the temporal portion of the ipsilateral retina. The largest density of NOT-DTN projecting ganglion cells was observed along a horizontal strip at the horizontal meridian. In case 1, the central ipsilateral retina was more densely labelled than the contralateral retina (Fig. 2). In addition, in a region around the optic disc of the contralateral retina (indicated by a circle), the ganglion cells were poorly labelled, probably due to remaining traces of vitreous body hampering the reaction of the chromogen TMB in this retina. Thus, to compensate for this, we omitted the cells located in the visuo-topically corresponding territory of the ipsilateral retina from the analysis. In contrast, in the other two animals, the highest density of the labelled ganglion cells was located between the fovea and the optic disc of the contralateral retina. On average, the contralateral retina contained two to three times more retrogradely labelled ganglion cells than the ipsilateral retina.

The number of the NOT-DTN projecting ganglion cells in each experiment is shown in Table 1. Although there was considerable variation of the total number of labelled ganglion cells, the ratio between ipsilaterally and contralaterally projecting ganglion cells (0.32–0.43) was similar in all three cases. The number of labelled ganglion cells roughly corresponded to the size of the injection. The Granular Blue injection in case 3 was certainly larger than the rhodamine–dextrane injection in case 2. The low numbers in case 1 can be explained by the exclusion of the central retina from the analysis (see above). In addition, efficiency may vary between tracers (Güntürkün *et al*., 1993). Comparing the number of labelled ganglion cells to the total number of ganglion cells in the retina and the number of axons in the optic nerve (Perry *et al*., 1984; Perry & Cowey, 1985), we found that on average 0.38%, and not more than 0.7%, of the ganglion cells project to the NOT-DTN. More specifically, on average 1.2–2.4% of the local ganglion cell population was labelled in the contralateral,

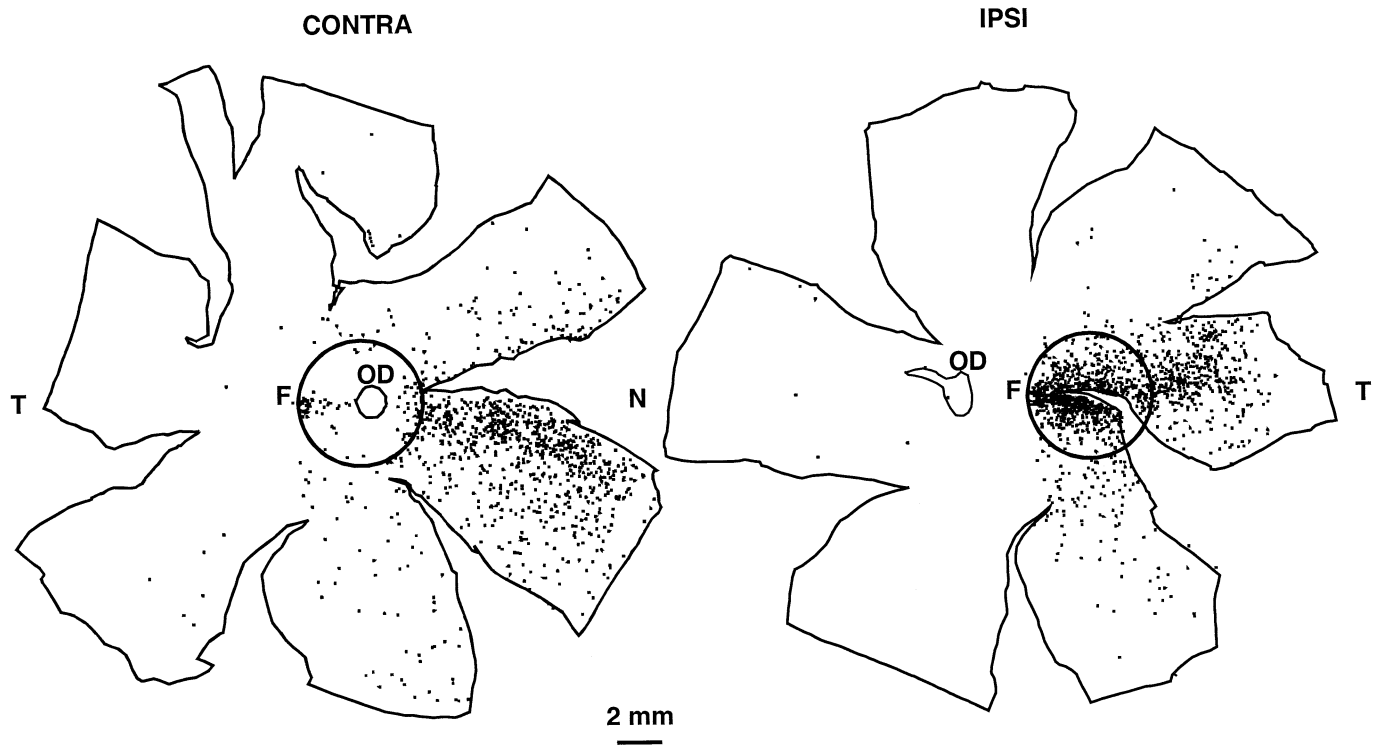

FIG. 2. Retrogradely labelled ganglion cells in the retinae of case 1 (*Macaca mulatta*) after a WGA-HRP/HRP injection into the right NOT-DTN. The circles indicate the area of poorly labelled cells in the contralateral retina and the corresponding area in the ipsilateral retina. These retinal regions were excluded from the quantitative analysis. F, fovea; OD, optic disc; T, temporal; N, nasal. Scale bar, 2 mm.

and 0.7–2.8% of the local ganglion cell population was labelled in the ipsilateral retina after NOT-DTN injection.

In Fig. 3 the density of retrogradely labelled ganglion cells at different retinal eccentricities (solid lines) along the fovea-optic disc line is compared with the overall ganglion cell density along the same line (according to Wässle *et al*., 1989; broken lines, ratio of number of labelled cells : total number of cells). The data from the contralateral (left row) and ipsilateral retina (right row) are plotted separately. Note that in case 1 (Fig. 3A) the central retina could not be analysed (see above). Because in case 3 (Fig. 3C) the labelling in the ipsilateral retina was restricted to a small region only, the data were not plotted in Fig. 3. As also demonstrated in Fig. 2, the highest density of retrogradely labelled ganglion cells occurred 2–3 mm from the fovea. However, even here the labelled ganglion cells represent only a very small proportion of the total number of ganglion cells present in this region. With increasing eccentricity the density of labelled cells declines, however, representing a slightly higher proportion of the overall ganglion cell population.

Soma size and classification of NOT-DTN projecting retinal ganglion cells

In all retinae, the vast majority of the labelled cells had cell bodies at the smaller end of the range of retinal ganglion cells as described by Perry *et al*. (1984). The soma size distribution of NOT-DTN projecting ganglion cells is shown in Fig. 4. Almost all somal areas were between 30 and 200μm^2; only a few cells were larger than 200μm^2 and, thus, were probably Pα-cells.

In the HRP-labelled retinae (case 1) we measured the soma size at various distances from the fovea. The fluorescent label in case 2 and 3 was not strong enough to allow correct measurement of soma size. Figure 5 shows the soma size of retrogradely labelled cells at different eccentricities. At larger eccentricities the cell sizes increased, only in the far periphery did we find large ganglion cells with cell body sizes similar to Pα cells.

In our material, most of the labelled ganglion cell dendrites were not sufficiently filled with tracer to allow reconstruction of the dendritic tree and thus unequivocally classify the cells. However, in some cells at least the stem dendrites were visible. In this restricted sample the most commonly encountered ganglion cells had small cell bodies and an extensive but sparsely branched dendritic tree. The filled dendrites were usually thin and smooth, and originated from single or more primary dendrites (Fig. 6A and B). We called these Pγ-like ganglion cells (Boycott & Wässle, 1974).

Some of the labelled cells in the far periphery had larger cell bodies than the majority of Pγ cells, but also had a large and sparsely branched dendritic tree (Fig. 6B and C). We called these Pε cells (Leventhal *et al*., 1980; Stone & Clarke, 1980).

Retrogradely labelled Pα-like ganglion cells (termed A cells by Leventhal *et al*., 1981 or parasol by Watanabe & Rodieck, 1989 and Rodieck & Watanabe, 1993) were only found in the far periphery of the retinae. These cells had ovoid or pyramidal cell bodies > 200 μm^2 and medium-sized, characteristic dendritic fields (Fig. 6D). Multiple fine dendrites arose from a few large coarse primary dendrites. Some of these cells in the HRP-labelled retinae had thick and well-defined axons that could be followed over several millimetres.

Discussion

The present study demonstrates that there is both a crossed and an uncrossed retinal projection to monkey NOT-DTN that originates mainly from the central region along the horizontal meridian of the retina. However, at 1–6% of the total, the ganglion cells projecting to the NOT-DTN represent a small proportion of the overall ganglion cell population at a certain eccentricity.

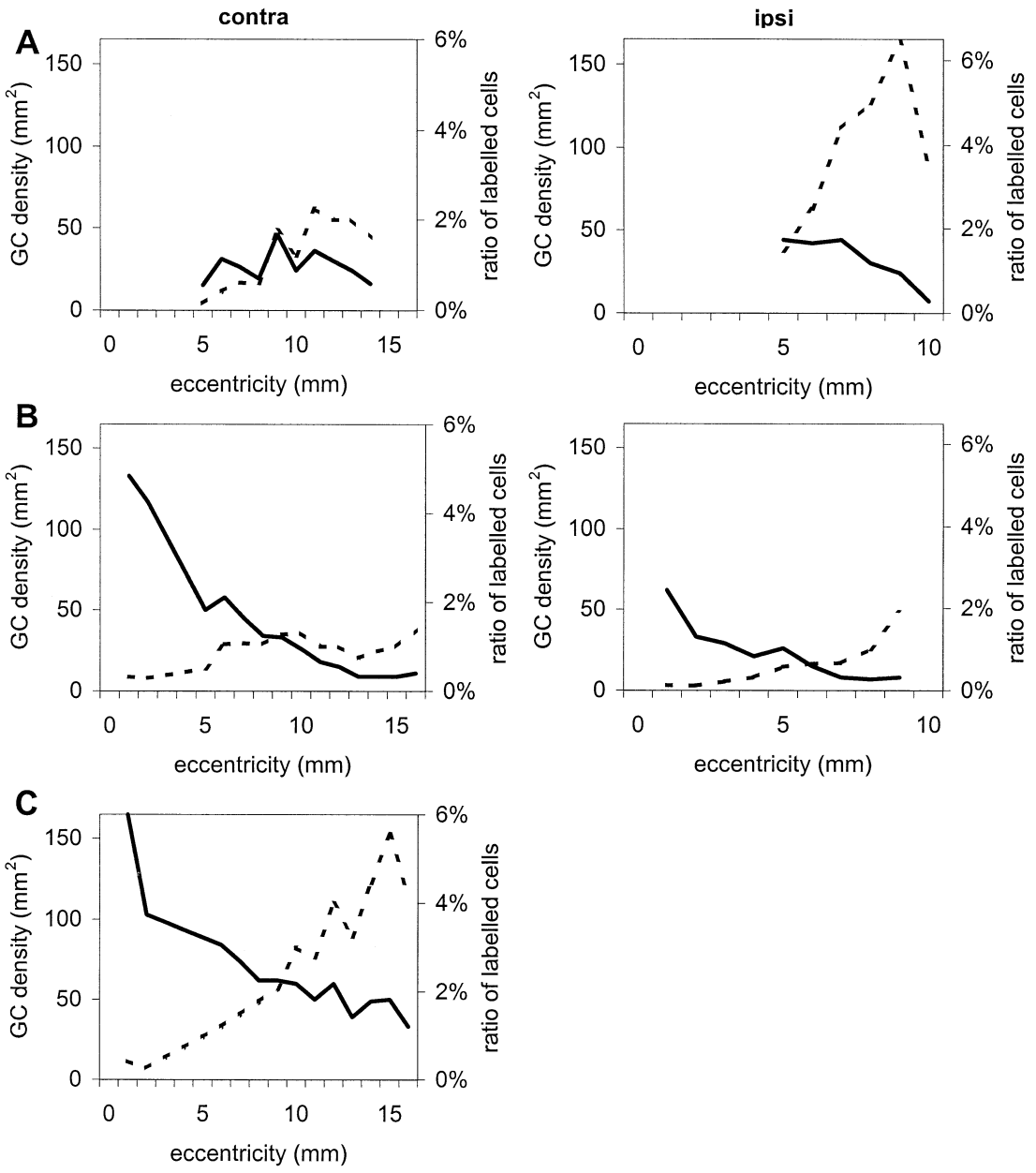

FIG. 3. The density of retrogradely labelled cells (cells/mm^2; left ordinate, solid line) and the ratio of labelled and total ganglion cell densities (right ordinate) (broken line) at different eccentricities along the horizontal meridian (abscissa). The data from the contralateral (left row) and the ipsilateral retinae (right row) are shown separately. (A) Case 1; (B) Case 2; (C) Case 3. The poorly labelled territory in case 1 was omitted from the density calculations, i.e. we started counting the cells at 5 mm eccentricity. Due to the spatially restricted labelling around the fovea in the ipsilateral retina of case 3 the data were not plotted. The data of the total number of retinal ganglion cells were taken from Wässle *et al.* (1989).

Injection sites

In the present study we aimed to reveal the number, distribution and type of ganglion cells projecting to the NOT-DTN. Because of the anatomical location of the NOT-DTN there are certain limitations to be considered. First, the pretectum is covered by ganglion cell axons projecting to the SC, so labelling of ganglion cells by an unspecific uptake of the tracer by fibres of passage cannot be wholly excluded (Bunt *et al.*, 1975; Rodieck, 1998). Secondly, the NOT-DTN is embedded in the BSC, and merges with the stratum opticum of the SC. Thus, some of the labelled ganglion cells could project to the SC. Therefore, even though the electrophysiologically controlled injections were unquestionably administered into the NOT-DTN, involvement of fibres of passage projecting to the SC or to other pretectal nuclei cannot be completely ruled out, even when WGA-HRP was used as the tracer. Nevertheless, all injections were clearly centred in the NOT-DTN so that the contribution of collicular or pretectal involvement should be minor. In addition, there was little or no labelling in the dorsal part of the retinae that should have been labelled by involvement of the lateral SC where the ventral visual field is represented. Involvement of the pulvinar into the area of spread of the tracer can be largely ruled out in cases 2 and 3, and was judged to be minor, if present at all, in case 1. Thus, it is unlikely that our data were contaminated by retinal projection to the pulvinar (Cowey *et al.*, 1994).

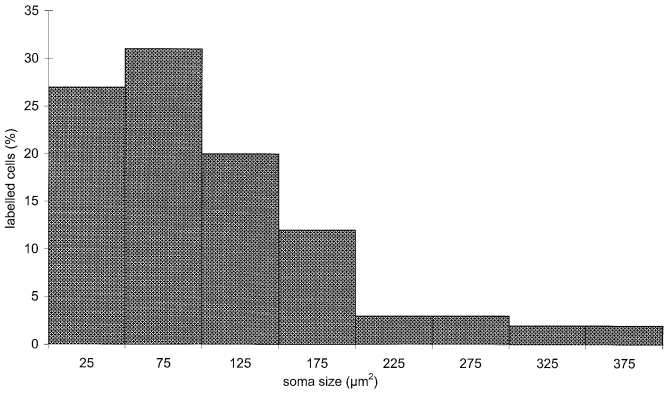

FIG. 4. Distribution of the soma size of NOT-DTN projecting ganglion cells in the HRP labelled retinae in case 1. The vast majority of the labelled cell bodies had an area of 30–200 μm², few somata exceeded 200μm². Ordinate, percentage of labelled ganglion cells; abscissa, soma size (μm²).

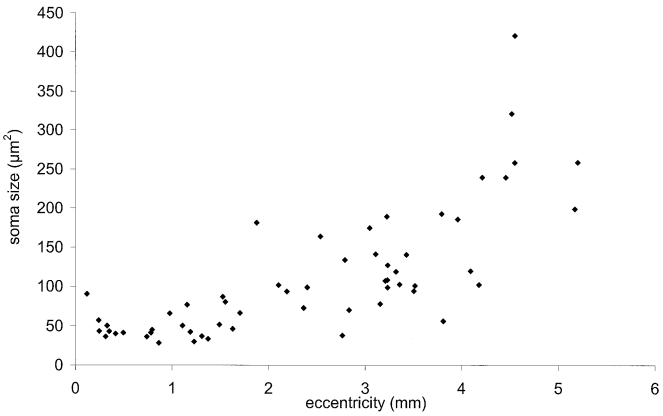

FIG. 5. Soma size (μm²; ordinate) of NOT-DTN projecting ganglion cells in case 1 in relation to the retinal eccentricity (mm, abscissa). Soma size increases with increasing eccentricity, large Pα-like ganglion cells (300–450 μm²) are only found in the periphery.

Distribution of NOT-DTN projecting ganglion cells

Similar to the overall decussation pattern of the macaque retina we found NOT-DTN projecting ganglion cells mainly in the temporal part of the ipsilateral retina and in the nasal section of the contralateral retina, with the highest density along the horizontal meridian. Confirming earlier studies, retrogradely labelled cells were found in overlapping regions of the fovea of both the contralateral and the ipsilateral retina (Stone *et al*., 1973; Fukuda *et al*., 1989). Very few individual cells (<< 1 cell/mm²) were found in the far nasal part of the ipsilateral and in the far temporal area of the contralateral retina (Fig. 2). Such cells were also identified by Perry & Cowey (1984) who considered them as morphogenetic accidents of no physiological relevance.

The density of labelled ganglion cells was highest close to the fovea and declined with increasing eccentricity. In contrast, the ratio of retrogradely labelled ganglion cells in relation to the overall number of retinal ganglion cells slightly increased with increasing eccentricity. This result can be viewed in relation to the fact that the peripheral visual field, in addition to the central visual field, is important for eliciting optokinetic eye movements, a behaviour for which the NOT-DTN is the key visuomotor interface (Buettner *et al*., 1983). To calculate the percentage of labelled ganglion cells at a certain eccentricity we referred to ganglion cell densities previously measured by Wässle *et al*. (1989). However, the peak ganglion cell density calculated in that particular study was almost twofold higher than that calculated by Perry & Cowey (1985). Thus, the data shown in Fig. 3 represent a minimal estimate, the maximal estimate could be much higher and thus lie in the vicinity of ganglion cells projecting to the SC (6–10%, Perry & Cowey, 1984). The overall comparison of labelled cells in the ipsilateral and contralateral retina showed a ratio between 0.32 and 0.43, thus confirming the anterograde tracing studies by Cooper *et al*. (1990) and Kourouyan & Horton (1997) that demonstrate the strong ipsilateral retinal projection to the midbrain, pretectum and AOS characteristic of primates.

Classification of NOT-DTN projecting ganglion cells

A clear classification of the NOT-DTN projecting ganglion cells is only possible to a limited extent with our current data. In most of the retrogradely labelled ganglion cells, especially in the small-sized cells in our material, the tracer was restricted to the soma and the dendrites were not labelled to a degree that would allow unequivocal analysis of their number, degree and shape of ramification, etc. This prevented not only any attempts of strict classification based on fine analysis of the dendritic tree but also a correlation of soma size and number of primary dendrites as used by Williams *et al*. (1995) for classification of ganglion cells. For a clear classification of the NOT-DTN projecting ganglion cell types one would have to intracellularly inject ganglion cells retrogradely prelabelled by tracer injections into the NOT-DTN, a method very successfully used in other studies (e.g. Pu & Amthor, 1990; Rodieck & Watanabe, 1993; Stein *et al*., 1996; Berson *et al*., 1999). Unfortunately, this approach was not possible because well-fixed brain tissue had to be shared with other projects. Nevertheless, by comparing our limited data with other studies, we can speculate on the nature of NOT-DTN projecting ganglion cells.

Similar to data in the cat, we found very few Pα-like ganglion cells in the far retinal periphery (Ballas *et al*., 1981) suggesting that this cell class does not play a crucial role for the direct retinal input to the AOS.

Soma sizes of NOT-DTN projecting ganglion cells in our study clearly overlap with the soma size of ganglion cells projecting to the SC or the pretectum (Rodieck & Watanabe, 1993). Most retrogradely labelled ganglion cells were characterized by small somata and, if visible at all, an extensive but sparsely branched dendritic tree. According to the description by Boycott & Wässle (1974) we called these cells Pγ-like ganglion cells. Many of these cells might correspond to the C cells discussed by Leventhal *et al*. (1981), described as having small cell bodies, fine axons, and very large dendritic fields.

In the far retinal periphery we encountered cells with relatively large cell bodies and a large and sparsely branched dendritic tree.

FIG. 6. Retinal ganglion cells retrogradely labelled with WGA-HRP/HRP from the NOT-DTN. (A) Pγ-like ganglion cells. The relatively small cell bodies with sparsely branching dendrites lie in the ganglion cell layer 8.8 mm nasal from the fovea. The dendrites arise from a single or a few primary dendrites (arrow). (B) A Pγ- (arrowhead) and a Pε-like (arrow) ganglion cell lying close to each other. Their distance from the fovea was 6.8 mm nasally. (C) Pε-like ganglion cells. The somata are larger than the Pγ-cells and have sparsely branching large dendritic fields. The cells lie 11.4 mm from the fovea in the contralateral retina. (D) Pα-like ganglion cell with a pyramidal cell body of 350μm² in the far nasal contralateral retina (10.9 mm from the fovea). Many finer dendrites (arrowheads) arise from a few large coarse primary dendrites (arrows). Scale bars, 50 μm.

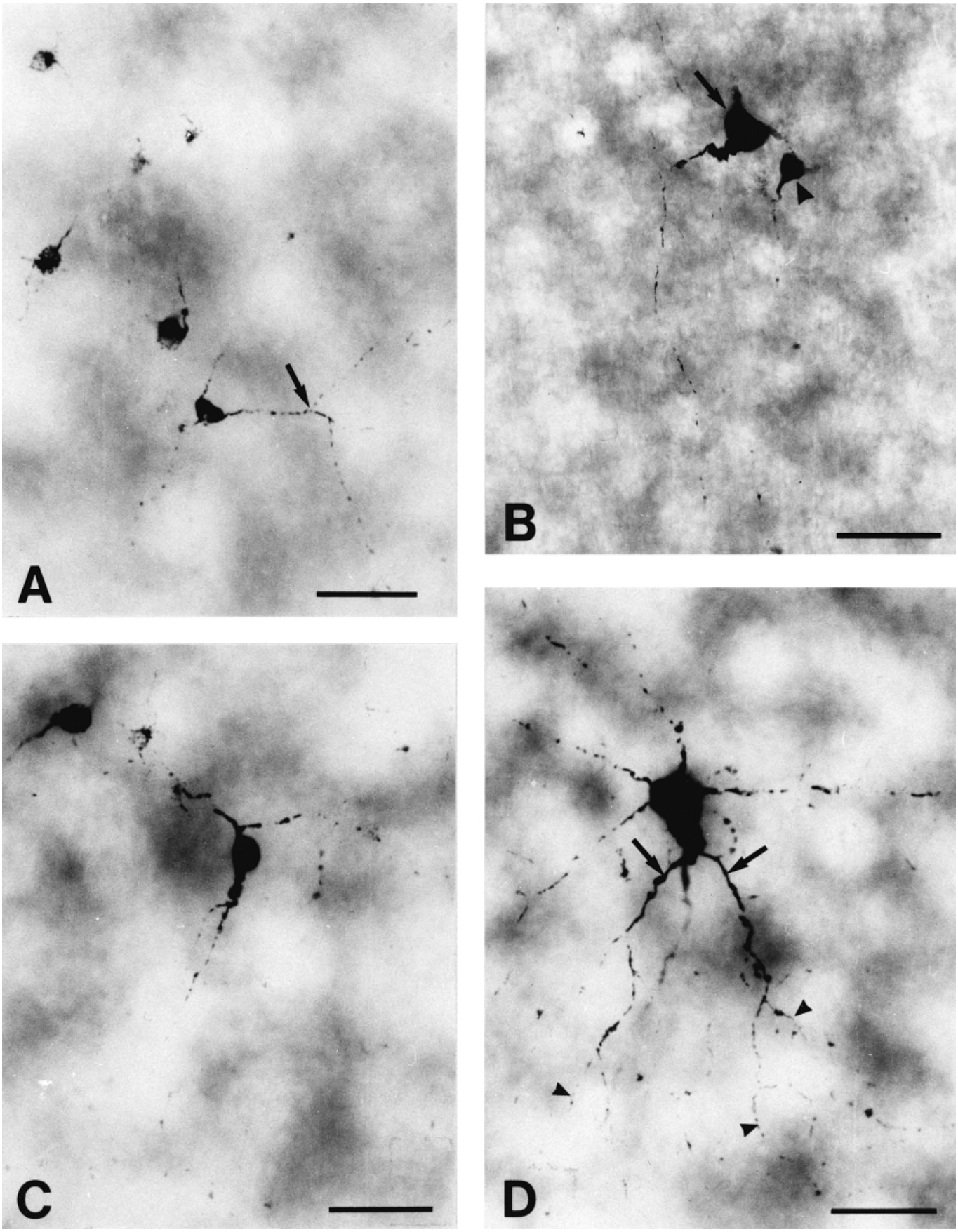
A
B
C
D

These cells might correspond to the Pε cells in the cat (Leventhal *et al*., 1980; Stone & Clarke, 1980) or the E cells (Leventhal *et al*., 1981) or 'PT-sparse' ganglion cells that project to the pretectum and have large, sparse and unistratified dendritic fields (Rodieck & Watanabe, 1993).

Thus, the majority of retinal ganglion cells projecting to the NOT-DTN may be classified as Pε- and Pγ-like ganglion cells. Nevertheless, this classification may be artificial because Rodieck & Watanabe (1993), using intracellular injection of prelabelled ganglion cells, argue that many if not all of the cells termed C, E, Pα and Pε may represent incompletely filled cells of other classes. Specifically, they show that monkey retina indeed contains Pα and Pε cells but that neither project to the SC or the pretectum. This dilemma cannot be solved using our present approach but, together with the physiological characterization of NOT-DTN projecting ganglion cells, awaits further morphological investigation.

Comparison with other species

Our data, together with earlier findings on the conduction velocity of retinal fibres projecting to the NOT-DTN (Hoffmann *et al*., 1988), indicate that in monkey, like in other vertebrates, the direct retinal input to the NOT-DTN and the pathway underlying the optokinetic reflex is provided by slowly conducting ganglion cells with small to medium-sized somata and large sparse dendritic trees [specialized cells in monkey, W-cells in cat, rabbit and rat (Ballas *et al*., 1981; Pu & Amthor, 1990; Kato *et al*., 1992; Rodieck & Watanabe, 1993)]. Studies in vertebrates as different as turtle, rabbit and cat have shown that retinal ganglion cells projecting to the AOS are direction selective (Oyster *et al*., 1972; Hoffmann & Stone, 1985; Rosenberg & Ariel, 1991). Comparable data from the monkey are not yet available. This is mainly due to technical reasons; the cells under consideration are small and the proportion of ganglion cells projecting to the NOT-DTN is low (< 1% of the total ganglion cell population, 1–6% of the local population, this study). Thus the probability of recording NOT-DTN projecting cells is slim.

Nevertheless, by extrapolating findings from subprimate species to the monkey one may assume that indeed direction selective ganglion cells exist in the primate retina, and that these ganglion cells may significantly contribute to the direction selectivity of retinal slip cells in the NOT-DTN during early development, as has been shown by experiments in cats (Distler & Hoffmann, 1993).

Functional interpretation

The most significant finding of the present study is the strong bilateral retinal input to the NOT-DTN in monkey. Our data, also supported by the anterograde studies by Cooper *et al*. (1990) and Kourouyan & Horton (1997), show that the retinal input from the ipsilateral eye is almost half as strong as that from the contralateral eye. Recently, we have demonstrated that in monkey monocular horizontal optokinetic nystagmus (hOKN) can be elicited both in a temporonasal and nasotemporal direction shortly after birth (Distler *et al*., 1999). This is unlike findings in the cat, where monocular hOKN can first be elicited only in the temporonasal direction. Electrophysiological studies indicate that in cat a symmetrical hOKN coincides with the occurence of a functional cortical input rendering the NOT-DTN binocular at 4 weeks of age (van Hof-van Duin, 1978; Malach *et al*., 1981). This cortical input balances the almost exclusively contralateral direct retinal input to the NOT-DTN (ipsilateral : contralateral, 1 : 10; Ballas *et al*., 1981; Distler & Hoffmann, 1993). In monkey, the optokinetic system appears more adult-like at birth. At that time, a high proportion of retinal slip cells in the NOT-DTN is already binocular (Distler & Hoffmann, 1998). To date, nothing is known about the development of the cortical input to the NOT-DTN in baby monkeys. However, our present data together with the anterograde tracing results in infant monkeys (Cooper *et al*., 1990; Kourouyan & Horton, 1997) open up the possibility that the bilateral direct retinal input to monkey NOT-DTN may be capable of supporting binocular reactions in the NOT-DTN that lead to a symmetrical hOKN, at least temporarily until the cortical input takes over. In adult monkeys, finally, the cortical input is more than 10-times greater than the retinal input to the NOT-DTN, which explains the devastating effect of decortication on OKN (Zee *et al*., 1987; Hoffmann *et al*., 1988). A similar developmental course has been implied by findings in human infants with excessive cortical damage (Morrone *et al*., 1999). These infants show monocular optokinetic reactions in both directions during the early postnatal period. At about 10 months of age, presumably at the time when the cortical input should normally take over the function of the retinal input, OKN is lost.

Acknowledgements

We wish to thank E. Brockmann and H. Korbmacher for technical assistance, and S. Krämer for photography. This study was supported by Sonderforschungsbereich SFB 509 of the Deutsche Forschungsgemeinschaft and a Lise Meitner stipend to C. Distler.

Abbreviations

AOS, accessory optic system; BSC, brachium of the superior colliculus; DPC, decussatio pedunculorum; DTN dorsal terminal nucleus of the accessory optic system; F, fovea; FLM fasciculus longitudinalis medialis; hOKN, horizontal optokinetic nystagmus; HRP, horseradish peroxidase; LL, lemniscus lateralis; NOT, nucleus of the optic tract; OD, optic disc; OKN, optokinetic nystagmus; PCM, pedunculus cerebellaris medius; PFA, paraformaldehyde; PLP, paraformaldehyde–lysine–periodate; PUL, pulvinar; SC, superior colliculus; TMB, tetramethylbenzidine; TP, tractus pyramidalis; WGA-HRP, wheatgerm agglutinin conjugated to horseradish peroxidase.

References

Ballas, I., Hoffmann, K.-P. & Wagner, H.-J. (1981) Retinal projection to the nucleus of the optic tract in the cat as revealed by retrograde transport of horseradish peroxidase. *Neurosci. Lett.*, **26**, 197–202.

Berman, N. (1977) Connections of the pretectum in the cat. *J. Comp. Neurol.*, **174**, 227–254.

Berson, D.M., Isayama, T. & Pu, M. (1999) The eta ganglion cell type of cat retina. *J. Comp. Neurol.*, **408**, 204–219.

Buettner, U., Meienberg, O. & Schimmelpfennig, B. (1983) The effect of central retinal lesions on optokinetic nystagmus in the monkey. *Exp. Brain Res.*, **52**, 248–256.

Boycott, B.B. & Wässle, H. (1974) The morphological types of ganglion cells of the domestic cat's retina. *J. Physiol. Lond.*, **240**, 397–419.

Bunt, A.H., Hendrickson, A.E., Lund, J.S., Lund, R.D. & Fuchs, A.F. (1975) Monkey retinal ganglion cells: morphometric analysis and tracing of axonal projections with a consideration of the peroxidase technique. *J. Comp. Neurol.*, **164**, 265–286.

Cooper, H.M., Baleydier, C. & Magnin, M. (1990) Macaque accessory optic system: I. Definition of the medial terminal nucleus. *J. Comp. Neurol.*, **302**, 394–404.

Cowey, A., Stoerig, P. & Bannister, M. (1994) Retinal ganglion cells labelled from the pulvinar nucleus in macaque monkeys. *Neuroscience*, **61**, 691–705.

Distler, C. & Hoffmann, K.-P. (1993) Visual receptive field properties in kitten pretectal nucleus of the optic tract and dorsal terminal nucleus of the accessory optic tract. *J. Neurophysiol.*, **70**, 814–827.

Distler, C. & Hoffmann, K.-P. (1998) Response properties of retinal slip neurons in the nucleus of the optic tract (NOT-DTN) in baby monkey. *Eur. J. Neurosci.*, **10** (Suppl 10), 188.

Distler, C., Vital-Durand, F., Korte, R., Korbmacher, H. & Hoffmann, K.-P. (1999) Development of the optokinetic system in macaque monkeys. *Vision Res.*, **39**, 3909–3919.

Fukuda, Y., Sawai, H., Watanabe, M., Wakakuwa, K. & Morigiwa, K. (1989)

Nasotemporal overlap of crossed and uncrossed retinal ganglion cell projections in the japanese monkey (Macaca fuscata). *J. Neurosci.*, **9**, 2353–2373.

Güntürkün, O., Melsbach, G., Hörster, W. & Daniel, S. (1993) Different sets of afferents are demonstrated by the fluorescent tracers Fast Blue and Rhodamine. *J. Neurosci. Meth.*, **49**, 103–111.

Hoffmann, K.-P. (1983) Control of the optokinetic reflex by the nucleus of the optic tract in the cat. In Hein, A. & Jeannerod, M. (eds), *Spatially Oriented Behavior.* Springer, New York, pp. 135–153.

Hoffmann, K.-P., Ballas, I. & Wagner, H.-J. (1984) Double labelling of retinofugal projections in the cat: a study using anterograde transport of ^{3}H-proline and horseradish peroxidase. *Exp. Brain Res.*, **53**, 420–430.

Hoffmann, K.-P. & Distler, C. (1989) Quantitative analysis of visual receptive fields of neurons in the nucleus of the optic tract and the dorsal terminal nucleus of the accessory optic tract in macaque monkeys. *J. Neurophysiol.*, **62**, 416–428.

Hoffmann, K.-P., Distler, C., Erickson, R. & Mader, W. (1988) Physiological and anatomical identification of the nucleus of the optic tract and dorsal terminal nucleus of the accessory optic tract in monkeys. *Exp. Brain. Res.*, **69**, 635–644.

Hoffmann, K.-P. & Stone, J. (1985) Retinal input to the nucleus of the optic tract of the cat assessed by antidromic activation of ganglion cells. *Exp. Brain Res.*, **59**, 395–403.

Kato, I., Okada, T., Watanabe, S., Sato, S., Urushibata, T. & Takeyama, I. (1992) Retinal ganglion cells related to optokinetic nystagmus in the rat. *Acta Otolaryngol. (Stockh.)*, **112**, 421–428.

Kourouyan, H.D. & Horton, J.C. (1997) Transneuronal retinal input to the primate Edinger-Westphal nucleus. *J. Comp. Neurol.*, **381**, 68–80.

Leventhal, A.G., Keens, J. & Törk, I. (1980) The afferent ganglion cells and cortical projections of the retinal recipient zone (RRZ) of the cat's 'pulvinar complex'. *J. Comp. Neurol.*, **194**, 535–554.

Leventhal, A.G., Rodieck, R.W. & Dreher, B. (1981) Retinal ganglion cell classes in old-world monkey: morphology and central projections. *Science*, **213**, 1139–1142.

Malach, R., Strong, N. & van Sluyters, R. (1981) Analysis of monocular optokinetic nystagmus in normal and visually deprived kittens. *Brain Res.*, **210**, 367–372.

Mesulam, M.-M. (1978) Tetramethylbenzidine for horseradish peroxidase neurohistochemistry: a non-carcinogenic blue reaction product with superior sensitivity for visualisation of neuron afferents and efferents. *J. Histochem. Cytochem.*, **26**, 123–131.

Morrone, M.C., Atkinson, J., Cioni, G., Braddick, O.J. & Fiorentini, A. (1999) Developmental changes in optokinetic mechanisms in the absence of unilateral cortical control. *Neuroreport*, **10**, 2723–2729.

Oyster, C.W., Takahashi, E. & Collewijn, H. (1972) Direction-selective retinal ganglion cells and control of optokinetic nystagmus in the rabbit. *Vision Res.*, **12**, 183–193.

Perry, V.H. & Cowey, A. (1984) Retinal ganglion cells that project to the superior colliculus and pretectum in the macaque monkey. *Neuroscience*, **12**, 1125–1137.

Perry, V.H. & Cowey, A. (1985) The ganglion cell and cone distributions in the monkey's retina: implications for central magnification factors. *Vision Res.*, **25**, 1795–1810.

Perry, V.H., Oehler, R. & Cowey, A. (1984) Retinal ganglion cells that project to the dorsal lateral geniculate nucleus in the macaque monkey. *Neuroscience*, **12**, 1101–1123.

Pu, M. & Amthor, F.R. (1990) Dendritic morphologies of retinal ganglion cells projecting to the nucleus of the optic tract in the rabbit. *J. Comp. Neurol.*, **302**, 657–674.

Rodieck, R.W. (1998) *The First Steps in Seeing*. Sinauer Associates, Inc., Sunderland, MA, USA.

Rodieck, R.W. & Watanabe, M. (1993) Survey of the morphology of macaque retinal ganglion cells that project to the pretectum, superior colliculus, and parvicellular laminae of the lateral geniculate nucleus. *J. Comp. Neurol.*, **338**, 289–303.

Rosenberg, A.F. & Ariel, M. (1991) Electrophysiological evidence for a direct projection of direction-selective retinal ganglion cells to the turtle's accessory optic system. *J. Neurophysiol.*, **65**, 1022–1033.

Simpson, J.I., Giolli, R.A. & Blanks, R.H.I. (1988) The pretectal nuclear complex and the accessory optic system. In Buettner-Ennever, J.A. (ed), *Neuroanatomy of the Oculomotor System.* Elsevier, Amsterdam, pp. 335–364.

Snider, R.S. & Lee, J.C. (1961) *A Stereotaxic Atlas of the Monkey Brain (Macaca mulatta)*. The University of Chicago Press, Chicago.

Stein, J.J., Johnson, S.A. & Berson, D.M. (1996) Distribution and coverage of beta cells in the cat retina. *J. Comp. Neurol.*, **372**, 597–617.

Stone, J. & Clarke, C. (1980) Correlation between soma size and dendritic morphology in cat retinal ganglion cells. Evidence for further variation in the γ-cell class. *J. Comp. Neurol.*, **192**, 211–218.

Stone, J., Leicester, J. & Sherman, S.M. (1973) The naso-temporal division of the monkey's retina. *J. Comp. Neurol.*, **150**, 333–348.

Szabo, J. & Cowan, W.M. (1984) A stereotaxic atlas of the brain of the cynomolgous monkey (Macaca fascicularis). *J. Comp. Neurol.*, **222**, 265–300.

Van der Want, J.J.L., Klooster, J., Nunes Cardozo, B., de Weerd, H. & Liem, R.S.B. (1997) Tract-tracing in the nervous system of vertebrates using horseradish peroxidase and its conjugates: tracers, chromogens, and stabilisation for light and electron microscopy. *Brain Res. Protocols*, **1**, 269–279.

van Hof-van Duin, J. (1978) Direction preference of optokinetic responses in monocularly tested normal kittens and light deprived cats. *Arch. Ital. Biol.*, **116**, 471–477.

Wässle, H., Grünert, U., Röhrenbeck, J. & Boycott, B.B. (1989) Cortical magnification factor and the ganglion cell density of the primate retina. *Nature*, **341**, 643–646.

Watanabe, M. & Rodieck, R.W. (1989) Parasol and midget ganglion cells of the primate retina. *J. Comp. Neurol.*, **289**, 434–454.

Williams, C., Azzopardi, P. & Cowey, A. (1995) Nasal and temporal retinal ganglion cells projecting to the midbrain: implications for 'blindsight'. *Neuroscience*, **65**, 577–586.

Zee, D.S., Tusa, R.J., Herdman, S.J., Butler, P.H. & Gücer, G. (1987) Effects of occipital lobectomy upon eye movements in primate. *J. Neurophysiol.*, **58**, 883–907.

Zhang, H.Y. & Hoffmann, K.-P. (1993) Retinal projections to the pretectum, accessory optic system and superior colliculus in pigmented and albino ferrets. *Eur. J. Neurosci.*, **5**, 486–500.